

Thermoelectric power of high- T_c superconductors

F. Devaux,* A. Manthiram, and J. B. Goodenough

Center for Materials Science and Engineering, ETC 5.160, University of Texas at Austin, Austin, Texas 78712

(Received 16 November 1989)

Thermoelectric-power measurements are reported for four copper oxide superconductor systems: $\text{La}_{2-y}\text{Sr}_y\text{CuO}_4$, $\text{Nd}_{1+y}\text{Ba}_{2-y}\text{Cu}_3\text{O}_{6+x}$, $\text{Y}_{0.6}\text{Ca}_{0.4}\text{Ba}_{1.6-y}\text{La}_{0.4+y}\text{Cu}_3\text{O}_{6+x}$, and $\text{Bi}_2\text{Sr}_{2-2y}\text{La}_{2y}\text{CuO}_{6+x}$. The Seebeck coefficient α is interpreted in terms of an electron-diffusion component α^e that varies from the small-polaron limit for the antiferromagnetic compositions to the metallic limit for the normal-metal compositions. It is argued that the width of the conduction band increases exponentially with oxidation of the CuO_2 sheets. At larger hole doping, the correlation splitting in the superconductor compositions becomes small enough to require the introduction of a two-band model for α^e . In those systems in which holes are trapped from the CuO_2 sheets into the "inactive" intergrowth layers, the temperature dependence of α develops a characteristic maximum at a temperature T_m . From a T^{-1} dependence for $T > T_m$, a trapping energy is extracted; this energy increases linearly with the formal charges of the intergrowth layers. The fall in α with decreasing temperature for $T < T_m$ is interpreted to reflect the consequences of a freezing out of the displacements of the c -axis oxygen that are associated with charge transfer between the "active" and "inactive" superconductor layers.

INTRODUCTION

Despite extensive and intensive efforts to probe experimentally the high- T_c copper oxides, the thermoelectric-power (TEP) data have, with few exceptions, failed to record the variation with composition in a systematic manner; they also tend to be restricted to temperatures below 300 K. These limitations have made it difficult to establish a firm interpretation of the data.

The TEP has been investigated previously in the systems $\text{La}_{2-y}\text{Sr}_y\text{CuO}_{4+x}$ (Refs. 1-7), $\text{YBa}_2\text{Cu}_3\text{O}_{6+x}$ (Refs. 5-19), $\text{Y}_{1-z}\text{Pr}_z\text{Ba}_2\text{Cu}_3\text{O}_{6+x}$ ($0 \leq z \leq 1$) (Ref. 20), $\text{YBa}_2\text{Cu}_{3-\lambda}\text{Zn}_\lambda\text{O}_{6+x}$ (Refs. 21 and 22), and $\text{Nd}_{1.85}\text{Ce}_{0.15}\text{CuO}_4$ (Refs. 23 and 24). Only the latter compound has a negative Seebeck coefficient α below room temperature for the superconductor compositions. Although small negative values of α have been reported⁵ for a single-crystal sample in the system $\text{YBa}_2\text{Cu}_3\text{O}_{6+x}$, this result is probably due to chemical inhomogeneities. It now appears that the TEP for homogeneous samples is positive for all x .

Previous measurements on the system $\text{La}_{2-y}\text{Sr}_y\text{CuO}_{4+x}$ have established that, for $y=0$ with $x < 0.02$, the TEP is large ($\alpha > 300\mu\text{V/K}$), positive, and nearly temperature independent. Moreover, α decreases dramatically with increasing y , and there is strong evidence that, for $y=0.25$, α extrapolates to a negative value above room temperature. This latter observation has been noted^{11,12} to be evidence of two-band conduction.

A temperature-independent Seebeck coefficient invites interpretation in the perspective of the small-polaron expression²⁵ for the electron-diffusion component

$$\alpha^e \approx -(k/e)\ln[\beta(1-c)/c], \quad 1 \leq \beta \leq 2, \quad (1)$$

where c is the concentration of mobile charge carriers on

the set of sites available to them and the factor β enters where there is a spin degeneracy. Where there is no motional enthalpy for charge transfer between neighboring sites, all near neighbors become accessible to a mobile charge carrier and Eq. (1) reduces to

$$\alpha^e \approx -(k/e)\ln(\beta/c). \quad (1')$$

A large magnitude of α means a small concentration c of mobile holes in the CuO_2 planes. However, the lack of any magnetic-field dependence of α for superconductor samples^{5,26} has been interpreted⁵ to mean that Eq. (1) is inapplicable to the copper oxide superconductors. On the other hand, the variation of α with oxygen concentration in the $\text{YBa}_2\text{Cu}_3\text{O}_{6+x}$ system¹⁹ and the possibility of an important phonon drag² and/or of two-band conduction^{11,12} have prevented any firm interpretation of the available data.

We report herein TEP measurements on four systems: $\text{La}_{2-y}\text{Sr}_y\text{CuO}_4$, $\text{Nd}_{1+y}\text{Ba}_{2-y}\text{Cu}_3\text{O}_{6+x}$, $\text{Y}_{0.6}\text{Ca}_{0.4}\text{Ba}_{1.6-y}\text{La}_{0.4+y}\text{Cu}_3\text{O}_{6+x}$, lastly and $\text{Bi}_2\text{Sr}_{2-2y}\text{La}_{2y}\text{CuO}_{6+x}$. This study was motivated by two principal questions.

What information does the TEP provide concerning the evolution of the conduction band on passing from the antiferromagnetic to the normal-metal compositions?

Does the temperature dependence of the TEP provide information on the trapping of holes in the "inactive" CuO_x planes of the $\text{YBa}_2\text{Cu}_3\text{O}_{6+x}$ structure with $x > 1$?

EXPERIMENTAL

The Seebeck coefficient α was measured with a conventional direct current (DC) differential technique.^{27,28} Both thermal and electrical contact were established by pressing a disk-shaped sample between two finely pol-

TABLE I. Sample preparation methods.

Compound	First firing in air	Second firing in air	Annealing/Cooling
$\text{Nd}_{1+y}\text{Ba}_{2-y}\text{Cu}_3\text{O}_{6+x}$ $0 \leq y \leq 0.4$	920–950 °C 24 h	920–950 °C 15 h	450 to 200 °C O_2 , 60 h
$\text{Y}_{0.6}\text{Ca}_{0.4}\text{Ba}_{1.6y}$ $\text{La}_{0.4+y}\text{Cu}_3\text{O}_{6+x}$	920–950 °C 24 h	920–950 °C 15 h	450 to 200 °C O_2 , 60 h
$\text{La}_{2-y}\text{Sr}_y\text{CuO}_{4+x}$ $0 \leq y \leq 0.4$	900 °C 12 h	1110–1180 °C 24 h	1180 to 25 °C air, 4 h
$\text{Bi}_2\text{Sr}_{2-2y}\text{La}_{2y}\text{CuO}_{6+x}$ $0.3 \leq 2y \leq 1.0$	790 °C 6 h 860 °C 20 h	860 °C 20 h	860 to 100 °C air, 6 h

ished Pt disks. The holder was sealed in a quartz tube that, once filled with He, can be either heated in a furnace or cooled in liquid nitrogen. This configuration was designed to allow an easy interchange of samples compatible with a TEP measurement of reasonable precision (10% relative to the TEP of Pt) at both low and high temperatures. The setup was successfully tested on Au and Cu.²⁹

The samples were prepared from stoichiometric ratios of the oxides and/or carbonates; the reactants were ground, fired, reground, pelletized, and annealed/cooled in either air or 1 atm O_2 followed by slow cooling as specified in Table I. All the starting and final products were examined by powder x-ray diffraction with a Philips diffractometer; only those specimens that were single phase to x-ray diffraction were retained for further analysis. The final oxygen content was determined to within ± 0.02 oxygen per formula unit by iodometric titration.³⁰ Thermogravimetric analysis (TGA) was carried out with a Perkin-Elmer thermal-analysis system in either an oxygen or a nitrogen atmosphere. The value of T_c for each composition was checked by a low-temperature resistance measurement with a standard four-probe technique.

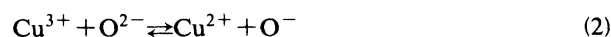
RESULTS AND DISCUSSION

A. $\text{La}_{2-y}\text{Sr}_y\text{CuO}_4$ system

The phase diagram for the system $\text{La}_{2-y}\text{Sr}_y\text{CuO}_4$ is illustrated in Fig. 1. The T -tetragonal structure consists of an intergrowth of CuO_2 planes and $\text{La}_{2-y}\text{Sr}_y\text{O}_2$ layers made up of two (001) rocksalt planes. Matching of the bond lengths across an interface encounters a thermal-expansion mismatch between the A -O and Cu-O bonds ($A = \text{La}$ or S) that increases with decreasing temperature. This mismatch, which decreases with increasing y , places the CuO_2 planes under a compressive stress, the $\text{La}_{2-y}\text{Sr}_y\text{O}_2$ layers under a tensile stress. It has three consequences:³¹ it orders the $3d$ -shell holes at a Cu^{2+} ion into $\sigma_{x^2-y^2}$ orbitals of $\text{Cu}-3d_{x^2-y^2}$ and $\text{O}-2p_{\sigma x}$, $2p_{\sigma y}$ parentage, it stabilizes the incorporation of excess oxygen in $\text{La}_2\text{CuO}_{4+x}$ annealed below 500 °C in air, and it induces a cooperative rotation of the CuO_6 octahedra along a [110] direction to give orthorhombic symmetry below a transition temperature T_t . The existence of a compres-

sive stress on the CuO_2 planes allows doping La_2CuO_4 p -type, especially with a larger Ba^{2+} or Sr^{2+} ion, but it inhibits n -type doping. With our thermal treatment, the compound $\text{La}_2\text{CuO}_{4+x}$ contains some oxygen excess ($x < 0.02$), but for $0 < y \leq 0.27$ the oxygen content is approximately stoichiometric in $\text{La}_{2-y}\text{Sr}_y\text{CuO}_4$. For $y > 0.27$, it is necessary to apply an oxygen pressure greater than 1 atm O_2 to obtain oxygen stoichiometry.^{32,33}

A striking feature of Fig. 1 is the occurrence of high- T_c superconductivity in a narrow compositional range between an antiferromagnetic-semiconductor and a normal-metal phase all within what appears structurally to be a single phase field. The transition from strong to weak electron correlations appears to be made possible by an equilibrium reaction



that is not biased too strongly to either the right or the left.³¹ Moreover, a closing of the correlation (Hubbard) splitting of the $\sigma_{x^2-y^2}$ band with increasing y results in a sharp decrease with y first in the long-range magnetic-ordering temperature T_N and then in the short-range spin fluctuations below a T_{max} , the temperature of a maximum in the magnetic susceptibility versus temperature. The

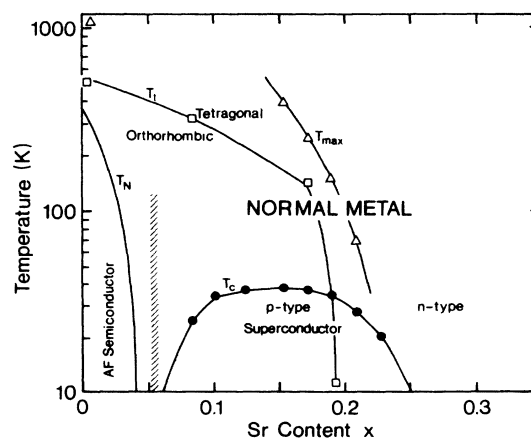


FIG. 1. Phase diagram for the system $\text{La}_{2-y}\text{Sr}_y\text{CuO}_4$. Adapted from Ref. 54.

copper moment of $0.5 \mu_B$ found in antiferromagnetic $\text{La}_2\text{CuO}_{4+x}$ (Ref. 34) apparently decreases with increasing y , disappearing in the normal-metal phase.

Figure 2 illustrates a proposed³¹ variation with y of the overlapping π^* and $\sigma_{x^2-y^2}^*$ bands; it accounts for the change from p -type to n -type conductivity—as determined by the room-temperature Hall effect³⁵—on passing from the superconductor to the normal-metal compositions. It includes the observation³⁶ of an “impurity” band developing at the top of the π^* band with increasing y . (Alternatively, the impurity band may be associated with the lower $\sigma_{x^2-y^2}^*$ band.) Placement of E_F within a narrow band in the superconductor compositional range has important implications for any theory of the coupling mechanism responsible for high- T_c superconductivity. Seebeck data provide a further test for an impurity-band model like that of Fig. 2, which appears to account qualitatively for the known structural, magnetic, optical, and spectroscopic data.³¹

Our TEP data for the system $\text{La}_{2-y}\text{Sr}_y\text{CuO}_4$, Fig. 3(a), are similar to those reported in the literature.¹⁻⁴ We confirm a large, positive, temperature-independent TEP for $\text{La}_2\text{CuO}_{4+x}$, $x < 0.02$. The anomaly near 280 K reflects the Néel temperature, which varies with the excess oxygen concentration over the range $240 \leq T_N \leq 326$ K.³⁷ A large anomaly at T_N has been observed earlier;⁴ it indicates the applicability of Eq. (1) in the antiferromagnetic compositions. From TGA, excess oxygen is lost above 500 K. Figure 3(a) also confirms the previously reported sharp drop in α with increasing y . In fact, Fig. 3(b) reveals an unusual exponential dependence on y of the room-temperature TEP. This plot, which includes points taken from the literature, is described by the relation

$$\alpha = 3.4(k/e)\exp(-y/y_c), \quad y_c = 0.055 \quad (3)$$

over the compositional range $0 \leq y \leq 0.27$; an oxygen deficiency is present for $y > 0.27$. Finally, since our data extends to higher temperatures, we are able to confirm that α does indeed change sign at higher temperatures for $y = 0.27$.

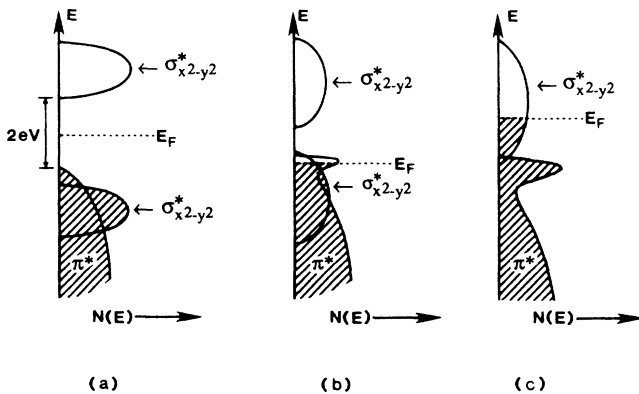


FIG. 2. Proposed evolution with y of the bands near the Fermi energy E_F for the system $\text{La}_{2-y}\text{Sr}_y\text{CuO}_4$. (a) $y=0$, (b) $y=0.15$, and (c) $y=0.4$ (Ref. 31).

We interpret the data in terms of the model of Fig. 2. This model shows two limiting phases: one is antiferromagnetic and the other is a normal metal. For the former, Eq. (1) is applicable to the electron-diffusion component; for the latter, the corresponding operating equation is the metallic expression³⁸

$$\alpha^e = -\frac{\pi^2 k}{3 e} \left[\frac{kT}{\zeta_0} \right] \left[\frac{3}{2} + \frac{d \ln \tau(E)}{d \ln E} \right], \quad (4)$$

where $\tau(E)$ is the relaxation (scattering) time of an electronic charge carrier of energy E , e is the magnitude of the electronic charge, and ζ_0 is the zero-temperature Fermi energy measured from the band edge (positive for electrons and negative for holes). In the intermediate, superconductive compositional range it is necessary to consider a two-band model in which the electron-diffusion component is given by³⁸

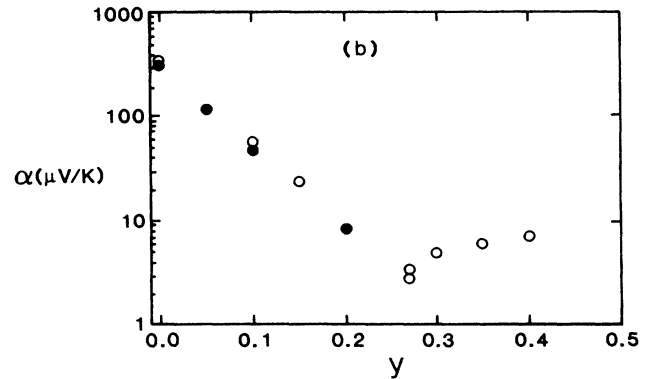
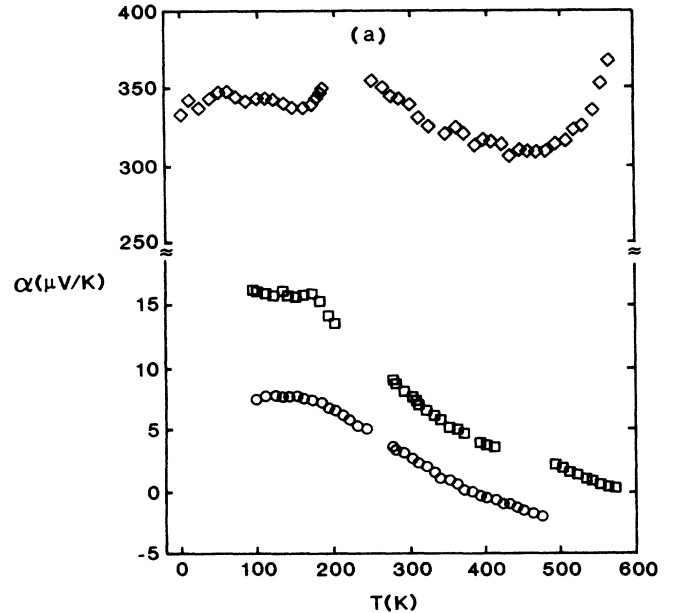


FIG. 3. Thermoelectric power α for the system $\text{La}_{2-y}\text{Sr}_y\text{CuO}_4$: (a) α vs temperature for different y ; diamonds, squares and circles refer, respectively, to $y=0.0$, 0.2 , and 0.27 . (b) room temperature α vs y . Solid circles refer to data from Refs. 1 and 2 and open circles refer to our data.

$$\alpha^e = (\alpha_1^e \sigma_1 + \alpha_2^e \sigma_2) / \sigma, \quad (5)$$

where $\sigma = \sigma_1 + \sigma_2$ is the sum of the conductivities from the valence and conduction bands and α_1^e, α_2^e are their respective Seebeck coefficients. For p -type superconductors the positive contribution would be roughly described by Eq. (4) whereas the negative contribution would be given by the nondegenerate semiconductor expression³⁸

$$a^e = + \frac{k}{e} \left[\frac{|\zeta|}{kT} + \frac{d \ln \tau(E)}{d \ln E} + \frac{5}{2} \right], \quad (6)$$

$$\zeta/kT = \ln(n/N_c), \quad N_c \equiv 2(2\pi m_n^* kT/h^2)^{3/2}, \quad (7)$$

where the concentration n of mobile electrons increases exponentially with the absolute temperature T .

The normal-state resistivity of antiferromagnetic $\text{La}_2\text{CuO}_{4+x}$ has been reported³⁹ to be nearly temperature independent, which is indicative of extrinsic conduction near the transition from small-polaron to itinerant-electron behavior where Eq. (1') is applicable. From Eq. (1'), the $\alpha > 300 \mu\text{V/K}$ in Fig. 3(a) is indicative of a small concentration c of mobile holes in the CuO_2 planes. On passing from Eq. (1') to Eq. (4), a small c corresponds to a small Fermi energy ζ_0 measured from, for $\alpha > 0$, the top of the valence band.

In the superconductor compositions $0.08 \leq y \leq 0.27$, the TEP rises abruptly from zero below T_c (not shown in our data) to a plateau in an interval $T_c < T < T'$. Above T' , either a negative contribution to α^e is introduced or an additional component (e.g., a phonon-drag component α^g) is decreasing with increasing temperature. The presence of a negative contribution is confirmed by the observation of a change in the sign of α at higher temperatures for the $y=0.27$ sample. Although a phonon-drag component $\alpha^g \sim 1/T$ may also be present, the data unambiguously reveal the presence of a negative component in α^e and hence are consistent with the two-band model of Fig. 2.

Within the context of only the electron-diffusion component α^e , the positive contribution should vary as kT/ζ_0 according to Eq. (4). Rationalization of Fig. 3 with Eq. (4) requires that ζ_0 decrease exponentially with the hole concentration y . There are two ways to think about how this might happen: either the number of sites available to a mobile hole or the bandwidth is changing exponentially with y . The former could occur for an impurity band. In the limit of Eq. (1'), for example, Eq. (3) follows if the ratio of mobile holes to the number of sites available to the holes is $c = y/y_f(y)$, where $f(y) = [1 - \exp(-y/y_c)]$. However, with such a model we could expect to find a decrease in c with increasing temperature, which would make α^e increase with temperature. Moreover, the fact that the system evolves from the narrow-band limit to the broad-band limit with increasing y clearly shows that the bandwidth is increasing with y . Therefore we focus on the second alternative since, in fact, ζ_0 varies not only with the hole concentration per band state, but also with the bandwidth.

If the hole concentration per band state does not decrease exponentially with y , it is necessary to have a band-

width that increases exponentially with increasing y to account for Eq. (3). In the tight-binding approximation, the bandwidth is $w \approx 2zb \approx \varepsilon_\sigma \lambda_\sigma^2$ where the number z of nearest neighbors is lumped with other factors into a one-electron energy ε_σ coming from the nearest-neighbor electron-transfer-energy integral $b_{ij} \equiv (\Psi_i, H' \Psi_j)$ associated with Cu-O-Cu interactions in the CuO_2 planes. The covalent-mixing parameter λ_σ entering the crystal-field wave function

$$\Psi_{x^2-y^2} = N_\sigma (d_{x^2-y^2} - \lambda_s \phi_s - \lambda_\sigma \phi_\sigma) \quad (8)$$

is defined by $\lambda_\sigma \equiv b^{ca}/\Delta$, where b^{ca} is the Cu-O electron-transfer-energy integral and Δ is the energy required to transfer an electron from the O- $2p_{\sigma_x}, 2p_{\sigma_y}$ orbitals to an empty Cu- $3d_{x^2-y^2}$ orbital. In (8), the orbitals ϕ_s and ϕ_σ are appropriately symmetrized O- $2s$ and O- $2p_{\sigma_x}, 2p_{\sigma_y}$ orbitals. In our qualitative discussion we neglect the contribution to w from $\lambda_s^2 < \lambda_\sigma^2$. In the copper oxide superconductors, a small Δ —because of Eq. (2)—makes λ_σ large. Moreover, the fact that the transition from a strongly correlated antiferromagnetic phase to a weakly correlated normal-metal phase occurs over a narrow range of oxidation states of the CuO_2 planes provides a clear indication that λ_σ increases dramatically with y . The matrix element b^{ca} contains an overlap integral for the Cu- $3d_{x^2-y^2}$ and O- $2p_{\sigma_x}, 2p_{\sigma_y}$ orbitals that increases exponentially with decreasing Cu-O distance, and this distance decreases with increasing y . Thus the parameter ζ_0 is seen to decrease exponentially with increasing y , and this decrease is enhanced by the fact that Δ is small. It follows that the positive contribution to α^e should decrease exponentially with y in qualitative agreement with the empirical formula (3).

The appearance of a negative contribution to α^e follows from the collapse of the correlation splitting with increasing y on traversing the superconductor compositional range; this collapse is indicated by the data of Fig. 1.³¹ However, narrow-band electrons generally experience a strong electron-lattice coupling in oxides, so we may also anticipate the presence of a phonon-drag component α^g at the narrower bandwidths (smaller y values). At temperatures $T > T'$, any α^g would decrease with increasing temperature $1/T$. This factor is deemed relatively unimportant for the present discussion.

In summary, we draw the following conclusions for the prototype system $\text{La}_{2-y}\text{Sr}_y\text{CuO}_4$.

(1) Equation (1) or (1') is applicable to the antiferromagnetic compositions; a remarkable change in α at T_N probably reflects a change in the parameter β .

(2) The normal-metal phase is expected^{31,40} to exhibit a negative Seebeck coefficient described by Eq. (4) in agreement with the Hall data.³⁵ The report³ of a positive α in a normal-metal phase prepared at 300 bar O_2 needs to be checked.

(3) The superconductor phase undergoes a transition with increasing y from a strongly correlated narrow-band metal to a weakly correlated metal; for temperatures $T > T'$, an intrinsic excitation of electrons from the p -type conduction band to the upper of the correlation-split $\sigma_{x^2-y^2}^*$ bands introduces a negative component described

by Eq. (6).

(4) The fact that the Seebeck coefficient is independent of an externally applied magnetic field indicates that the conduction electrons do not couple significantly to the spin fluctuations in the normal state of the superconductors. The fact that there is no change in the observed spin fluctuations on cooling through T_c (Ref. 41) would therefore suggest that the superconductive pairs do not interact with the short-range spin fluctuations.

(5) The remarkable exponential decrease with y in the positive component of α , Eq. (4), is consistent with an exponential increase with y of the bandwidth in the narrow superconductor compositional range.

(6) A phonon-drag component α^g may also be present in the superconductors; such a component is expected to decrease in magnitude with increasing width of the conduction bands and to be relatively unimportant at the temperatures investigated.

B. $\text{YBa}_2\text{Cu}_3\text{O}_{6+x}$ structures

The phase diagram for the system $\text{YBa}_2\text{Cu}_3\text{O}_{6+x}$, $0 \leq x < 1$, is shown in Fig. 4. In this system the intergrowths are a CuO_2 -Y-CuO₂ layer of fixed oxygen content and a BaO-CuO_x-BaO layer of variable oxygen content. The tetragonal-orthorhombic transition and the steplike rise in T_c with increasing x can be accounted for

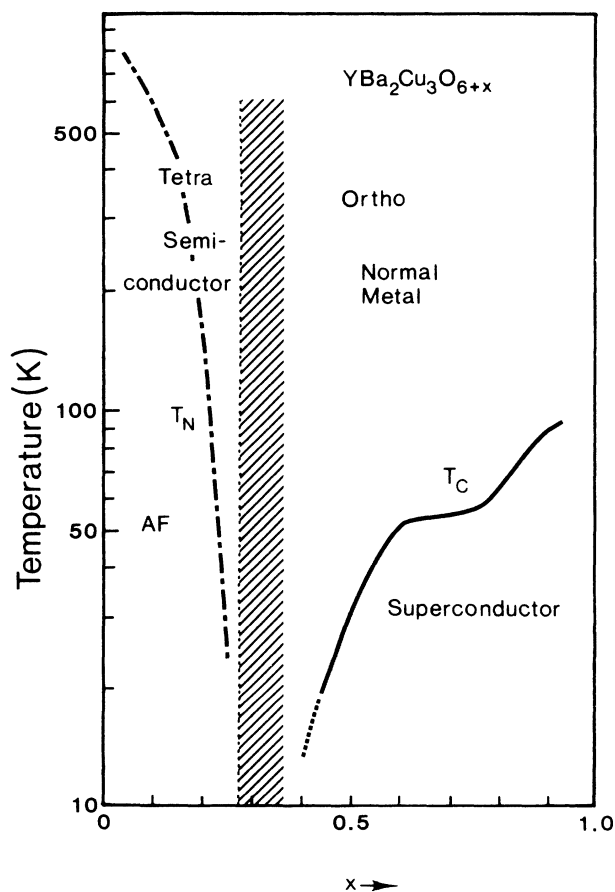


FIG. 4. Phase diagram for the system $\text{YBa}_2\text{Cu}_3\text{O}_{6+x}$.

by a preferential ordering of the oxygen in the CuO_x planes⁴² and the observation⁴³ that T_c is proportional to the concentration p of mobile holes in the CuO_2 -Y-CuO₂ layers. Comparison of Figs. 4 and 1 suggests that T_c has reached a maximum plateau in the interval $0.90 < x < 0.98$; in this case the addition of more holes in the CuO_2 -Y-CuO₂ layers would cause T_c to decrease with increasing x for $x > 1$. The first attempt⁴⁴ to demonstrate such a decrease with the system $\text{Y}_{1-z}\text{Ca}_z\text{Ba}_2\text{Cu}_3\text{O}_{6+x}$ was frustrated by an equilibrium oxygen concentration $x = 0.94 - 0.5z$ after an anneal at 400°C in 1 atm O₂. However, application of a high oxygen pressure to this system promises to increase the oxidation state of the CuO_2 planes within the context of an $x < 1$, and a muon-spin-rotation (μSR) study⁴³ appears to have included this system prepared under 300 bar O₂; the data indicate that T_c reaches its maximum value at $\text{YBa}_2\text{Cu}_3\text{O}_{6.96 \pm 0.02}$.

Substitution of Ln^{3+} ions for Ba^{2+} ions in 1 atm O₂ also leads to a constant oxidation state of the Cu-O array, as was shown independently for $\text{YBa}_{2-y}\text{La}_y\text{Cu}_3\text{O}_{6.87+0.5y}$ (Ref. 45) and $\text{NdBa}_{2-y}\text{Nd}_y\text{O}_{6.94+0.5y}$.⁴⁶ Nevertheless, T_c decreases linearly with $y \geq 0.1$ in both systems due to a trapping out of mobile holes from the CuO_2 planes to the inactive $\text{Ba}_{1-0.5y}\text{Ln}_{0.5y}\text{O-CuO}_x$ - $\text{Ba}_{1-0.5y}\text{Ln}_{0.5y}\text{O}$ layers. X-ray photoelectron spectroscopy (XPS) data⁴⁷ have shown that the holes are trapped in oxygen-atom clusters, which we presume are centered at the oxygen atoms on a -axis sites. Although a peroxide species $(\text{O}_2)^{2-}$ was originally postulated, recent neutron-diffraction data⁴⁸ indicate that two holes may be trapped at two copper sites adjacent to the a -axis oxygen in a large Cu_2O_9 cluster. A subsequent study^{49,50} has shown that in the codoped system $\text{Ca}_z\text{Y}_{1-z}\text{Ba}_{2-z-y}\text{La}_{z+y}\text{Cu}_3\text{O}_{6+x}$, there is a critical value of $y = y_c$ for a given value of z above which trapping out of mobile holes is initiated. The dependence of y_c on z is due to the dependence on z of the magnitude of the internal c -axis electric field introduced by the formal charges on adjacent basal planes. The temperature dependence of the TEP provides a means of measuring the activation energies of these hole traps.

Figure 5(a) shows the temperature dependence of the Seebeck coefficient α for the system $\text{NdBa}_{2-y}\text{Nd}_y\text{Cu}_3\text{O}_{6+x}$, $x = 0.94 + 0.5y$, prepared under 1 atm O₂. For $y \geq 0.1$ in this system, $(x-1)$ oxygen atoms are forced to occupy a -axis sites of the CuO_x planes; these a -site oxygen atoms tend to be located adjacent to the Nd^{3+} ions substituting for Ba^{2+} ions. If the concentration of mobile holes in the active CuO_2 -Y-CuO₂ layers remained constant, we could expect a constant T_c independent of y . However, Fig. 5(b) shows that T_c is constant only in the interval $0 \leq y \leq 0.1$ where there are few, if any, oxygen on a -axis sites; for $y > 0.1$ the magnitude of T_c decreases with increasing y due to a trapping of holes at a -axis oxygen atoms in the CuO_x planes. Therefore we expect the Seebeck data to show evidence for the trapping out of holes with an activation energy that increases with the internal c -axis electric field, which would increase linearly with y .

For $0 \leq y \leq 0.1$, the Seebeck data of Fig. 5(a) are similar to those observed for the superconductor

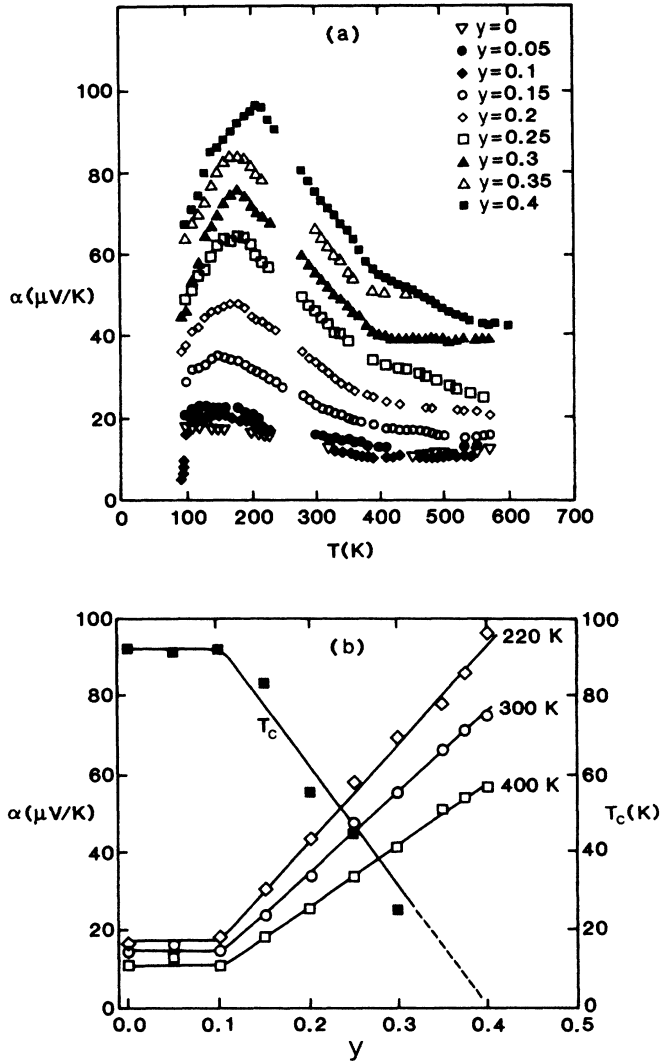


FIG. 5. Thermoelectric power α for the system $\text{Nd}_{1+x}\text{Ba}_{2-y}\text{Cu}_3\text{O}_{6+x}$, $x \approx 0.94 + 0.5y$. (a) α vs temperature for different y and (b) α vs y for different temperatures compared with T_c vs y . Open and solid symbols refer, respectively, to α and T_c .

$\text{La}_{1.8}\text{Sr}_{0.2}\text{CuO}_4$, Fig. 3(a), in which there is no hole trapping. For $y \geq 0.1$, the α vs T curves of Fig. 5(a) show a maximum α at a T_m ; this maximum grows larger and is shifted to higher temperatures with increasing y . The resistance below room temperature shows no anomaly in its temperature variation at T_m ; however, it changes from an itinerant character with strong electron-phonon coupling (linear increase with T) to a small-polaron character (activated mobility) at $y \approx 0.2$. This observation shows that the bandwidth decreases with increasing y in this system.

At the composition $y=0$, α^e is described by Eq. (4). An increase in α with decreasing temperature has been noted by several workers in the interval $T_c < T \lesssim 150$ K; some attribute it to phonon drag,^{2,4,11} but anomalies in the sound velocity⁵¹ and volume⁵² in this same temperature interval would support the argument by others^{10,12}

that a major contribution is due to superconductive-pair fluctuations (short-range pairing) just above T_c .

With increasing y , a decreasing bandwidth correlates with the introduction of a -axis oxygen into the CuO_x planes, and for $y > 0.2$ the bands may be narrow enough for Eq. (1') to apply. At these compositions, a maximum in α at $T = T_m$ grows with increasing y , and at $T > T_m$ we find that α varies as $1/T$. Hall data⁴⁶ signal a trapping out of mobile holes from the CuO_2 sheets to the CuO_x planes for $y > 0.2$, and the concentration of holes trapped out appears to saturate at about two per a -axis oxygen.^{45,47} Within the context of Eq. (1'), the measured temperature variation of α for $T > T_m$ can be expected for a hole concentration $c = c_0 \exp(-E_a/kT)$. Moreover, Fig. 5(b) shows that, for any given temperature in the interval $T_m < T < 400$ K, α increases where T_c decreases with increasing y . Within the context of Eq. (1'), T_c is clearly correlated with the concentration c of mobile holes. The calculated temperature of activation $T_a \equiv E_a/k$ versus composition y is plotted in Fig. 6; it increases linearly with y for $T_a > T_c$. This result indicates that the holes are trapped in the inactive layers with a trapping energy that increases linearly with the strength of the internal c -axis electric field associated with the negative formal charge of a CuO_x plane. Any phonon-drag component would only make the measured activation energy an upper limit to the true E_a .

A surprising feature of Fig. 5(a) is the sharp decrease in α with decreasing temperature in the interval $T_c < T < T_m$. In order to account for this feature, a more detailed discussion of the trapping mechanism is required. We may assume that the trapping out of a mobile hole from a CuO_2 sheet to a CuO_x plane is accompanied by a displacement of a c -axis oxygen away from the CuO_2

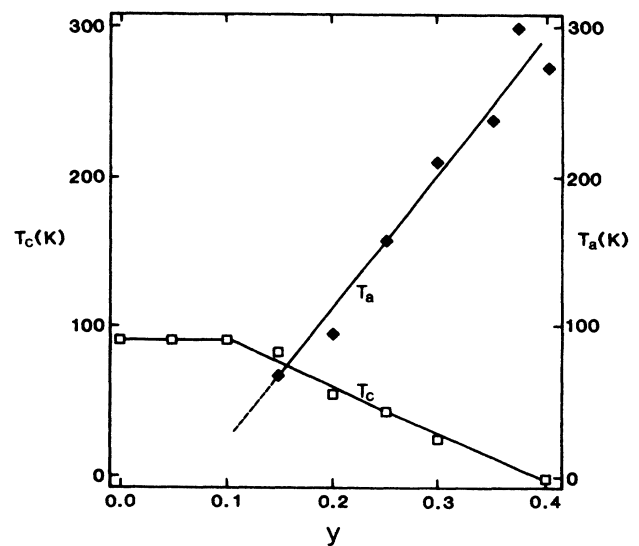


FIG. 6. Critical temperature T_c and activation temperature $T_a \equiv E_a/k$ vs y for the system $\text{Nd}_{1+x}\text{Ba}_{2-y}\text{Cu}_3\text{O}_{6+x}$, $x \approx 0.94 + 0.5y$. Open and solid squares refer, respectively, to T_c and T_a .

sheet toward the CuO_x plane. Such a displacement would raise the energy of a local antibonding state in the CuO_x plane so as to trap the hole; it would lower the local electron potential energy in the CuO_2 sheets so as to exclude access to that local region by the mobile holes in the CuO_2 sheets. It follows that if the displacements of the c -axis oxygen become frozen below T_m , then the number of sites in a CuO_2 sheet that are accessible to the holes decreases. A reduction in the number of accessible sites is equivalent, in the context of Eq. (1'), to an increase in the effective concentration of charge carriers c . (Note that the density of mobile holes remains constant.) In the context of Eq. (4), a freezing out of the oxygen displacements would broaden the width of the conduction band, thereby increasing ξ_0 and decreasing α , even if the Fermi energy remained above the mobility edge of the perturbed band. In this model, a dynamic capture of the mobile holes at temperatures $T > T_m$ leaves all sites accessible, but it narrows the bandwidth; it also introduces an activation energy E_a into the population of charge carriers.

The codoped system $\text{Y}_{0.6}\text{Ca}_{0.4}\text{Ba}_{1.6-y}\text{La}_{0.4+y}\text{Cu}_3\text{O}_{6+x}$ annealed in 1 atm O_2 shows a break in the T_c versus y curve at a $y_c \approx 0.3$ that was interpreted^{49,50} as the onset of hole trapping for $y > y_c$. It is gratifying that our interpretation of the α versus T curves in copper oxides with the $\text{YBa}_2\text{Cu}_3\text{O}_{6+x}$ structure support this conclusion. Figure 7 shows the α versus T curves we obtained for this system. For $y \leq 0.1$, the magnitude of α is typical of that for a broad-band metal with no important phonon-drag component. For $0.2 \leq y < y_c$ the curves are like those for $\text{La}_{1.8}\text{Sr}_{0.2}\text{CuO}_4$ in Fig. 3(a), which we interpreted in terms of Eq. (4). The introduction of a -axis oxygen into the CuO_x planes appears to narrow the width of the valence band, thereby reducing ξ_0 , even though it does not trap out holes from this band for $y \leq y_c$. The appearance of a

maximum in α at a $T = T_m$ that grows with increasing $y \geq 0.4$ is a confirmation that the appearance of a T_m coincides with the trapping out of mobile holes from the active layers and that such trapping only occurs for $y > y_c$.

C. $\text{Bi}_2\text{Sr}_{2-2y}\text{La}_{2y}\text{CuO}_{6+x}$, $x \approx 0.21 + 0.6y$ system

The structure of this system is similar to that of T -tetragonal La_2CuO_4 except for double sheets of $\text{Bi}_2\text{O}_{2+x}$ in the middle of the inactive rocksalt layer. Oxygen atoms in excess of O_6 are placed periodically along the b axis of the orthorhombic structure within the $\text{Bi}_2\text{O}_{2+x}$ double sheets;⁵³ these periodically placed oxygen atoms oxidize the single CuO_2 planes to make compositions with $2y < 0.7$ superconductors. Compositions with $2y \geq 0.7$ are antiferromagnetic semiconductors⁵⁰ even though the total hole concentration is *ca.* 0.15 per Cu atom at $2y = 0.7$, which suggests that at least some of these holes are trapped out from the CuO_2 sheets to the $\text{Bi}_2\text{O}_{2+x}$ layers.

TGA measurements show that these materials lose weight when first heated in an inert atmosphere; the substance lost is not pure oxygen since the sample does not regain weight on subsequent slow cooling in air. In order to avoid a thermal hysteresis of the TEP, it is necessary first to perform a full thermal cycle in an inert atmosphere. The TEP curves obtained after the first thermal cycle are shown in Fig. 8. For $2y \geq 0.6$, the TEP exhibits a maximum value at T_m with a $1/T$ dependence for $T > T_m$. The antiferromagnetic semiconductors apparently trap out mobile holes from the CuO_2 planes at lower temperatures, which places E_F above a mobility edge at the top of the valence band. The superconductor compositions have α vs T curves like those found for the superconductor compositions in $\text{La}_{2-y}\text{Sr}_y\text{CuO}_4$ where there is no mobile-hole trapping. Apparently substitution of La^{3+} ions for Sr^{2+} ions in $\text{Bi}_2\text{Sr}_{2-2y}\text{La}_{2y}\text{CuO}_{6+x}$ not

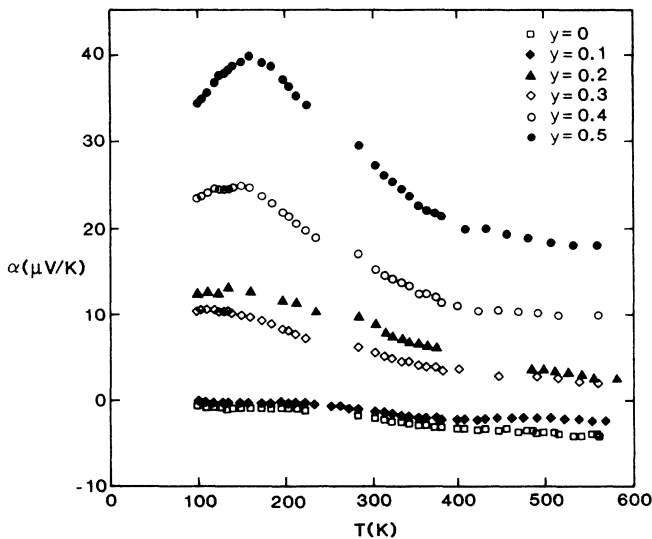


FIG. 7. Thermoelectric power α vs temperature for different y in the system $\text{Y}_{0.6}\text{Ca}_{0.4}\text{Ba}_{1.6-y}\text{La}_{0.4+y}\text{Cu}_3\text{O}_{6+x}$, $x \approx 0.75 + 0.5y$.

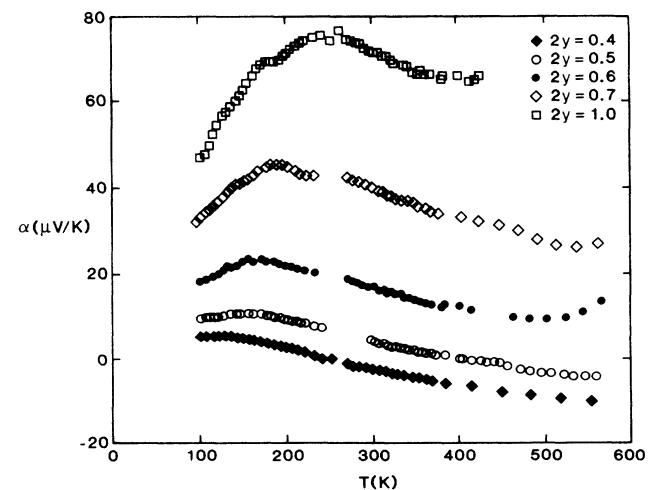


FIG. 8. Thermoelectric power α vs temperature for different y in the system $\text{Bi}_2\text{Sr}_{2-2y}\text{La}_{2y}\text{CuO}_{6+x}$, $x \approx 0.21 + 0.6y$.

only reduces the CuO_2 layers; it also narrows the conduction band, thereby decreasing ζ_0 in Eq. (4). The appearance of hole trapping for $2y \geq 0.6$ indicates that the La^{3+} ions also introduce interstitial, disordered oxygen into the $\text{Bi}_2\text{O}_{2+x}$ layers that can act as hole traps.

CONCLUSIONS

The preliminary TEP measurements reported above allow the following conclusions to be drawn.

(1) The width of the conduction band in the p -type copper oxide superconductors varies exponentially with the oxidation state of the superconductive CuO_2 sheets.

(2) Where mobile holes are trapped from the CuO_2 sheets into "inactive" layers, the temperature dependence of α develops a characteristic maximum at a temperature

T_m ; a T^{-1} dependence of α for $T > T_m$ allows extraction of an activation energy E_a , which appears to reflect the trapping energy. At temperatures $T < T_m$, c -axis displacements of the c -axis oxygen become frozen in; consequently for $T < T_m$ holes remain captures in the inactive layers, which reduces T_c . The number of sites available to the mobile holes is decreased and the bandwidth is increased with decreasing temperature for $T < T_m$.

ACKNOWLEDGMENTS

Support for the research by the Robert A. Welch Foundation, Houston, Texas and the Texas Advanced Research Program Grant No. 4257 is gratefully acknowledged.

*Also at the École Supérieure de Physique et Chimie Industrielles de Paris.

¹J. R. Cooper, B. Alavi, L.-W. Zhou, W. P. Beyermann, and G. Grüner, *Phys. Rev. B* **35**, 8794 (1987).

²C. Uher, A. B. Kaiser, E. Gmelin, and L. Walz, *Phys. Rev. B* **36**, 5676 (1987).

³Y. Ando, M. Sera, S. Yamagata, S. Kondoh, M. Onoda, and M. Sato, *Solid State Commun.* **70**, 303 (1989).

⁴S.-W. Cheong, M. F. Hundley, J. D. Thompson, and Z. Fisk, *Phys. Rev. B* **39**, 6567 (1989).

⁵R. C. Yu, M. J. Naughton, X. Yan, P. M. Chaikin, F. Holtzberg, R. L. Greene, J. Stuart, and P. Davies, *Phys. Rev. B* **37**, 7963 (1988).

⁶N. Mitra, J. Trefny, and M. Young, *Phys. Rev. B* **36**, 5581 (1987).

⁷M. Sera, S. Shamoto, and M. Sato, *Solid State Commun.* **68**, 649 (1988).

⁸Z. G. Khim, S. C. Lee, J. H. Suh, Y. W. Park, C. Park, and I. S. Yu, *Phys. Rev. B* **36**, 2305 (1987).

⁹A. Mawdsley, H. J. Trodahl, J. Tallon, J. Sarfati, and A. B. Kaiser, *Nature London* **328**, 233 (1987).

¹⁰H. J. Trodahl and A. Mawdsley, *Phys. Rev. B* **36**, 8881 (1987).

¹¹Z. Henkie, R. Horyń, Z. Bukowski, P. J. Markowski, and J. Klamut, *Solid State Commun.* **64**, 1285 (1987).

¹²C. Uher and A. B. Kaiser, *Phys. Rev. B* **36**, 5680 (1987).

¹³N. P. Ong, Z. Z. Wang, S. J. Hagen, T. W. Jing, J. Clayhold and J. Horvath, *Physica* **153-155C**, 1072 (1988).

¹⁴M. Sera, S. Kondoh, and M. Sato, *Solid State Commun.* **68**, 647 (1988).

¹⁵M. N. Hlopkin, J. Toth, A. A. Sikov, and E. Zsoldos, *Solid State Commun.* **68**, 1011 (1988).

¹⁶Z. Z. Wang and N. P. Ong, *Phys. Rev. B* **38**, 7160 (1988).

¹⁷M. F. Crommie, A. Zettl, T. W. Barbee III, and M. L. Cohen, *Phys. Rev. B* **37**, 9734 (1988).

¹⁸Z. Henkie, P. J. Markowski, R. Horyń, Z. Bukowski, and J. Klamut, *Phys. Status Solidi B* **146**, 131 (1988).

¹⁹J. Genossar, B. Fisher, I. O. Lelong, Y. Ashkenazi, and L. Patlagan, *Physica C* **157**, 320 (1989).

²⁰A. P. Gonçalves, I. C. Santos, E. P. Lopes, R. T. Henriques, M. Almeida, and M. O. Figueiredo, *Phys. Rev. B* **37**, 7476 (1988).

²¹H. Zhenkui, Z. Han, S. Shifang, C. Zuyao, Z. Qirui, and X. Jiansheng, *Solid State Commun.* **66**, 1215 (1988).

²²V. Radhakrishnan, C. K. Subramanian, V. Sankaranarayanan, G. V. Subba Rao, and R. Srinivasan, *Phys. Rev. B* **40**, 6850 (1989).

²³M. E. Lopez-Morales, R. J. Savoy and P. M. Grant, *Solid State Commun.* **71**, 1079 (1989).

²⁴Z. S. Lim, K. H. Han, S.-I. Lee, Y. H. Jeong, S. H. Salk, Y. S. Song, and Y. W. Park, *Phys. Rev. B* **40**, 7310 (1989).

²⁵P. M. Chaikin, *Phys. Rev. B* **13**, 647 (1976).

²⁶Ch. Laurent, S. K. Patapis, M. Laguesse, H. W. Vanderschueren, A. Rulmont, P. Tarte, and M. Ausloos, *Solid State Commun.* **66**, 445 (1988).

²⁷P. H. Klein, in *Thermoelectricity*, edited by P. H. Egli (Wiley, New York 1960), p. 257.

²⁸B. Poumelle, F. Marcellet, F. Lagnel, and J. F. Marucco, *J. Phys. E* **21**, 159 (1988).

²⁹F. Devaux, M. S. thesis, The University of Texas at Austin, 1989.

³⁰A. Manthiram, J. S. Swinnea, Z. T. Sui, H. Steinfink, and J. B. Goodenough, *J. Am. Chem. Soc.* **109**, 6667 (1987).

³¹J. B. Goodenough, *Supercond. Sci. Technol.* **3**, 26 (1990).

³²M. W. Shafer, T. Penney, and B. L. Olson, *Phys. Rev. B* **36**, 4047 (1987).

³³J. B. Torrance, Y. Tokura, A. I. Nazzal, A. Bezinge, T. C. Huang, and S. S. P. Parkin, *Phys. Rev. Lett.* **61**, 1127 (1988).

³⁴D. Vaknin, S. K. Sinha, D. E. Moncton, D. C. Johnston, J. M. Newsam, C. R. Safinya, and H. E. King, Jr., *Phys. Rev. Lett.* **58**, 2802 (1987).

³⁵H. Takagi, S. Uchida, and Y. Tokura, *Mater. Res. Soc. Symp.* **156**, 389 (1989).

³⁶M. Tachiki, *Proceedings of the Tsukuba Seminar on High T_c Superconductivity, Tsukuba, Japan, 1989*, edited by K. Masuda, T. Arai, I. Iguchi, and R. Yoshizaki (University of Tsukuba, Tsukuba, 1989), p. 45.

³⁷S.-W. Cheong, J. D. Thompson, and Z. Fisk, *Physica C* **158**, 109 (1989).

³⁸D. K. C. MacDonald, *Thermoelectricity: An Introduction to the Principles* (Wiley, New York, 1962).

³⁹P. Ganguly and C. N. R. Rao, *Mater. Res. Bull.* **8**, 405 (1973).

⁴⁰J. B. Goodenough, A. Manthiram, and J. Zhou, *Mater. Res. Soc. Symp.* **156**, 339 (1989).

⁴¹R. J. Birgeneau, D. R. Gabbe, H. P. Jenssen, M. A. Kastner, P. J. Picone, T. R. Thurston, G. Shirane, Y. Endoh, M. Sato, K. Yamada, Y. Hidaka, M. Oda, Y. Enomoto, M. Suzuki,

- and T. Murakami, Phys. Rev. B **38**, 6614 (1988).
- ⁴²C. J. Hou, A. Manthiram, L. Rabenberg, and J. B. Goodenough, J. Mater. Res. **5**, 9 (1990).
- ⁴³Y. J. Uemura *et al.*, Phys. Rev. Lett. **62**, 2317 (1989).
- ⁴⁴A. Manthiram, S.-J. Lee, and J. B. Goodenough, J. Solid State Chem. **73**, 278 (1988).
- ⁴⁵A. Manthiram, X. X. Tang, and J. B. Goodenough, Phys. Rev. B **37**, 3734 (1988).
- ⁴⁶K. Takita, H. Akinaga, H. Katoh, H. Asano, and K. Masuda, Jpn. J. Appl. Phys. **27**, L67 (1988).
- ⁴⁷Y. Dai, A. Manthiram, A. Campion, and J. B. Goodenough, Phys. Rev. B **38**, 5091 (1988).
- ⁴⁸M. Izumi, T. Yabe, T. Wada, A. Maeda, K. Uchinokura, S. Tanaka, and H. Asano, Phys. Rev. B **40**, 6771 (1989).
- ⁴⁹A. Manthiram, and J. B. Goodenough, Physica C **159**, 760 (1989).
- ⁵⁰A. Manthiram, and J. B. Goodenough, Physica **162-164C**, 69 (1989).
- ⁵¹D. P. Almond, E. Lambson, G. A. Saunders, and W. Hong, J. Phys. F **17**, L221 (1987).
- ⁵²R. Srinivasan, K. S. Girirajan, V. Ganesan, V. Rhadakrishnan, and G. V. Subba Rao, Phys. Rev. B **38**, 889 (1988).
- ⁵³Y. Le Page, W. R. McKinnon, J. -M. Tarascon, and P. Barboux, Phys. Rev. B **40**, 6810 (1989).
- ⁵⁴J. B. Torrance, A. Bezing, A. I. Nazzari, T. C. Huang, and S. S. P. Parkin, Phys. Rev. B **40**, 8872 (1989).